

This discussion paper is/has been under review for the journal Earth System Dynamics (ESD). Please refer to the corresponding final paper in ESD if available.

# Two-dimensional prognostic experiments for fast-flowing ice streams from the Academy of Sciences Ice Cap: future modeled histories obtained for the reference surface mass balance

Y. V. Konovalov and O. V. Nagornov

Mathematical Department, National Research Nuclear University “MEPhI”,  
Kashirskoe shosse, 31, 115409 Moscow, Russian Federation

Received: 13 October 2015 – Accepted: 19 October 2015 – Published: 3 November 2015

Correspondence to: Y. V. Konovalov (yu-v-k@yandex.ru)

Published by Copernicus Publications on behalf of the European Geosciences Union.

ESDD

6, 2211–2242, 2015

## Fast-flowing ice streams from the Academy of Sciences Ice Cap

Y. V. Konovalov and  
O. V. Nagornov

Title Page

Abstract

Introduction

Conclusions

References

Tables

Figures

◀

▶

◀

▶

Back

Close

Full Screen / Esc

Printer-friendly Version

Interactive Discussion



## Abstract

The prognostic experiments for fast-flowing ice streams on the southern side of the Academy of Sciences Ice Cap in the Komsomolets Island, Severnaya Zemlya archipelago, are implemented in this study. These experiments are based on inversions of basal friction coefficients using a two-dimensional flow-line thermo-coupled model and the Tikhonov's regularization method. The modeled ice temperature distributions in the cross-sections were obtained using the ice surface temperature histories that were inverted previously from the borehole temperature profiles derived at the Academy of Sciences Ice Cap. Input data included InSAR ice surface velocities, ice surface elevations, and ice thicknesses obtained from airborne measurements and the surface mass balance, were adopted from the prior investigations for the implementation of both the forward and inverse problems. The prognostic experiments reveal that both ice mass and ice stream extents decline for the reference time-independent surface mass balance. Specifically, the grounding line retreats (a) along the B–B' flow line from ~ 40 to ~ 30 km (the distance from the summit), (b) along the C–C' flow line from ~ 43 to ~ 37 km, and (c) along the D–D' flow line from ~ 41 to ~ 32 km considering a time period of 500 years and assuming time-independent surface mass balance. Ice flow velocities in the ice streams decrease with time and this trend results in the overall decline of the outgoing ice flux. Generally, the modeled histories are in agreement with observations of sea ice extent and thickness indicating a continual ice decline in the Arctic.

## 1 Introduction

There are relevant diagnostic observations of glaciers such as digital Landsat imagery and satellite synthetic aperture radar interferometry (InSAR), airborne measurements, borehole ice temperature and ice surface mass balance measurements. These observations provide data for prognostic experiments that allow prediction of future glacier

# ESDD

6, 2211–2242, 2015

## Fast-flowing ice streams from the Academy of Sciences Ice Cap

Y. V. Konovalov and  
O. V. Nagornov

Title Page

Abstract

Introduction

Conclusions

References

Tables

Figures

◀

▶

◀

▶

Back

Close

Full Screen / Esc

Printer-friendly Version

Interactive Discussion



## Fast-flowing ice streams from the Academy of Sciences Ice Cap

Y. V. Konovalov and  
O. V. Nagornov

Title Page

Abstract

Introduction

Conclusions

References

Tables

Figures

◀

▶

◀

▶

Back

Close

Full Screen / Esc

Printer-friendly Version

Interactive Discussion



conditions for different climatic scenarios in the future. These experiments can be performed employing the mathematical modeling and in this study a two-dimensional ice flow model is applied for prediction of the future conditions of fast-flowing ice streams on the southern side of the Academy of Sciences Ice Cap in the Komsomolets Island, Severnaya Zemlya archipelago (Fig. 1; Dowdeswell et al., 2002).

The observations were based on digital Landsat imagery and satellite synthetic aperture radar interferometry (InSAR) and revealed four drainage basins and four fast-flowing ice streams on the southern side of the Academy of Sciences Ice Cap in the Komsomolets Island, Severnaya Zemlya archipelago (Fig. 2; Dowdeswell et al., 2002). The four ice streams are 17–37 km long and 4–8 km wide (Dowdeswell et al., 2002). Bedrock elevations of these areas are below the sea level, and the ice flow velocities attain a value of 70–100  $\text{m a}^{-1}$  (Fig. 2). Such fast flow-line features are typical for outlet glaciers and ice streams in both the Arctic and the Antarctic. These ice streams are the major locations of iceberg calving from the Academy of Sciences Ice Cap (Dowdeswell et al., 2002).

The flow-line profiles of the three ice streams on the southern side of the Academy of Sciences Ice Cap are shown in Fig. 3. Ice flow in these ice streams is simulated with a two-dimensional flow-line finite-difference model (e.g. Colinge and Blatter, 1998; Pattyn, 2000, 2002). This model describes an ice flow along a flow line (Pattyn, 2000, 2002). The results of the diagnostic experiments obtained in Konovalov (2012), for instance, for the C–C' flow-line profile show that the ice surface velocity along the flow line attains a value of 100  $\text{m a}^{-1}$  assuming that ice is sliding. However, the observed surface velocity distribution along the C–C' flow-line profile (Dowdeswell et al., 2002) is not similar to that obtained by the model experiments for constant values of friction coefficient and for both linear and nonlinear friction laws (Konovalov, 2012). Similarly, the diagnostic experiments carried out for the B–B' and D–D' profile data show the same results for the ice flow velocities. The deviation between the observed and modeled surface velocities suggests that the friction coefficient should be a spatially variable parameter. Therefore, to achieve a better agreement between the observed and simulated

## Fast-flowing ice streams from the Academy of Sciences Ice Cap

Y. V. Konovalov and  
O. V. Nagornov

Title Page

Abstract

Introduction

Conclusions

References

Tables

Figures

◀

▶

◀

▶

Back

Close

Full Screen / Esc

Printer-friendly Version

Interactive Discussion



velocities, the spatial distribution of the friction coefficients requires to be optimized and an inverse problem needs to be solved (e.g. MacAyeal, 1992; Sergienko et al., 2008; Arthern and Gudmundsson, 2010; Gagliardini et al., 2010; Habermann et al., 2010; Morlighem et al., 2010; Jay-Allemand et al., 2011; Larour et al., 2012).

The inversion of friction coefficients is based on the minimization of the deviation between the observed and modeled surface velocities. A series of test experiments (Konovalov, 2012), in which modeled surface velocities are used as observations in the inverse problem, have shown that the inverse problem for the full 2-D ice flow-line model is ill posed. More precisely, the surface velocity is weakly sensitive to small perturbations in friction coefficients, and as a result the perturbations appear in the inverted friction coefficients (Konovalov, 2012).

Herein, we present a solution to the ill-posed inversion problem by applying the Tikhonov's regularization method, in which Tikhonov's stabilizing functional is added to the main discrepancy functional (Tikhonov and Arsenin, 1977).

The inversions of friction coefficient are used in the prognostic experiments for the fast-flowing ice streams. The considered 2-D prognostic experiments are the numerical simulations with the ice thickness distribution changes performed by the 2-D flow-line thermo-coupled model, which includes diagnostic equations as the heat-transfer equation and the mass-balance equation (Pattyn, 2000, 2002). In this study, we present the results of the prognostic experiments performed for the B–B', C–C', and D–D' profiles (Fig. 3). Specifically, the prognostic experiments are carried out for the three ice streams (Fig. 2) that are the main sources of the ice flux from the ice cap to the ocean. The results of the prognostic experiments include future modeled histories of ice thickness distributions along the flow lines of grounding line locations and outgoing ice fluxes. The surface mass balance in the performed experiments is considered as time-independent, so the prognostic experiments show the assessment of the maximal ice mass in the ice streams in the future, because the obtained forecasts do not imply a future global warming. Nevertheless, the results of the prognostic experiments are in

agreement with the observations of sea ice extent and thickness indicating a continual ice decline in the Arctic.

## 2 Field equations

### 2.1 Forward problem: diagnostic equations

5 The 2-D flow-line model includes the continuity equation for incompressible medium, the mechanical equilibrium equation in terms of stress deviator components (Pattyn, 2000, 2002), and the rheological Glen law (Cuffey and Paterson, 2010):

$$\left\{ \begin{array}{l} \int_{h_b}^z \frac{\partial u}{\partial x} dz' + \frac{1}{b} \frac{db}{dx} \int_{h_b}^z u dz' + w - w_b = 0, \\ 2 \frac{\partial \sigma'_{xx}}{\partial x} + \frac{\partial \sigma'_{yy}}{\partial x} + \frac{\partial^2}{\partial x^2} \int_z^{h_s} \sigma'_{xz} dz + \frac{\partial \sigma'_{xz}}{\partial z} = \rho g \frac{\partial h_s}{\partial x}, \\ \sigma'_{ik} = 2\eta \dot{\epsilon}_{ik}; \quad \eta = \frac{1}{2} (mA(T))^{-\frac{1}{n}} \dot{\epsilon}^{\frac{1-n}{n}}, \\ 0 < x < L; \quad h_b(x) < z < h_s(x), \end{array} \right. \quad (1)$$

10 where  $(x, z)$  is a rectangular coordinate system with the  $x$  axis along the flow line and the  $z$  axis pointing vertically upward;  $u$ ,  $w$  are the horizontal and vertical ice flow velocities, respectively;  $b$  is the width along the flow-line,  $\sigma'_{ik}$  is the stress deviator;  $\dot{\epsilon}_{ik}$  is the strain-rate tensor;  $\dot{\epsilon}$  is the second invariant of the strain-rate tensor;  $\rho$  is the ice density;  $g$  is the gravitational acceleration;  $\eta$  is the ice effective viscosity;  $A(T)$  is the flow-law rate factor;  $T$  is the ice temperature;  $h_b(x)$ ,  $h_s(x)$  are the ice bed and ice surface elevations, respectively; and  $L$  is the glacier length.

15 The boundary conditions and some complementary experiments that were carried out applying this model, were considered in Konovalov (2012).



## Fast-flowing ice streams from the Academy of Sciences Ice Cap

Y. V. Konovalov and  
O. V. Nagornov

Title Page

Abstract

Introduction

Conclusions

References

Tables

Figures

◀

▶

◀

▶

Back

Close

Full Screen / Esc

Printer-friendly Version

Interactive Discussion

where  $\chi$  and  $C$  are the thermal diffusivity and the specific heat capacity, respectively.

In this model it is suggested that the ice surface temperature at the Academy of Sciences Ice Cap varies with an elevational gradient of temperature changes, which is equal to about  $6.5 \text{ K km}^{-1}$ . Hence, the ice surface temperature distribution along the flow line is defined by the temperature history at the summit  $T_{s0}(t)$  and by the elevational changes, and it is expressed as

$$T_s(x, t) = T_{s0}(t) + \theta_T(h_s(0) - h_s(x)), \quad (4)$$

where  $\theta_T$  is the elevational gradient. Therefore, Eq. (4) provides the boundary condition on the ice surface.

The boundary condition at the ice base is defined by the geothermal heat flux and by the heating due to the basal friction, and it is expressed as (Pattyn, 2000, 2002)

$$\frac{\partial T}{\partial z} = -\frac{1}{k} (Q + (\sigma'_{xz})_b u_b), \quad (5)$$

where  $k$  is the thermal conductivity.

The boundary conditions at the ice (ice-shelf) terminus and at the ice-shelf base are defined by sea water temperature, which is considered as  $-2^\circ\text{C}$  in this study.

The ice thickness temporal changes along the flow line are described by the mass-balance equation (Pattyn, 2000, 2002):

$$\frac{\partial H}{\partial t} = M_s - M_b - \frac{1}{b} \frac{\partial(\bar{u}bH)}{\partial x}, \quad (6)$$

where  $\bar{u}$  is the depth-averaged horizontal velocity,  $M_s$  is the annual surface mass balance, and  $M_b$  is the melting rate at the ice base.

The mass-balance equation requires two boundary conditions at the summit and at the ice terminus. The first condition at the ice cap summit implies that  $\frac{\partial h_s}{\partial x} = 0$ . The second condition applied in the ice terminus originates from the fact that the ice thicknesses in the ice shelf along the flow line attain a constant value at the terminus.

### 3 Results of the numerical experiments

#### 3.1 Inversions for the friction coefficient

For the first run of the friction coefficient inversions, the linear ice temperature profile approximation is applied. Specifically, it is assumed that the ice temperature linearly increases from  $-15^{\circ}\text{C}$  at the surface to  $-5^{\circ}\text{C}$  at the ice base at the division and increases from  $-2$  to  $-1^{\circ}\text{C}$  at the grounding line. Figure 4a shows the inverted friction coefficient distribution along the C–C' flow line. The retrieved friction coefficient gradually decreases from  $\sim 3.5 \times 10^3 \text{ Pa a m}^{-1}$  to a mean value of  $5 \times 10^2 \text{ Pa a m}^{-1}$  within a distance of around  $25 \text{ km} < x < 40 \text{ km}$  (Fig. 4a). The difference between the simulated and *observed* surface velocities is relatively small (Fig. 4b).

The inverted friction coefficient distributions along the B–B' and D–D' flow lines show qualitatively the same trends, i.e. they gradually decrease along the flow line from a high to a lower level.

After the first run of the inversions, the ice temperature simulations are performed for inverted friction coefficients and boundary conditions (Eqs. 4 and 5). Boundary condition (Eq. 4) includes the temperature history  $T_{s0}(t)$ . In particular, if the history is the past temperature (Nagornov et al., 2005, 2006), which was inverted previously from the borehole temperature profile derived at the Academy of Sciences Ice Cap (Zagorodnov, 1988; Arkhipov, 1999), then we would expect the simulated output temperature close to the real present temperature in the ice stream along the flow line. In other words, the modeled temperature will be close to the present temperature (in the year when borehole measurements were performed), assuming a good agreement between the model results and the real physical processes that occur in the glacier, which are in general described by the model. The past surface temperature history, which was applied in the simulations of the present ice temperature, was adopted from Nagornov et al. (2005, 2006). The modeled present temperature distributions along the B–B', C–C' and D–D' cross-sections are shown in Fig. 5.

## Fast-flowing ice streams from the Academy of Sciences Ice Cap

Y. V. Konovalov and  
O. V. Nagornov

Title Page

Abstract

Introduction

Conclusions

References

Tables

Figures

◀

▶

◀

▶

Back

Close

Full Screen / Esc

Printer-friendly Version

Interactive Discussion



For the second run of the basal friction coefficient inversions, the modeled temperature distributions are applied. The inverted friction coefficients (i) for the linearly approximated ice temperature and (ii) for the modeled ice temperature are shown in Fig. 6. Generally, the distinctions in the friction coefficients are insignificant, and, therefore, the ice temperature approximations can be applied in the inverse problem as the first iteration of the ice temperature distribution in the glacier.

### 3.2 Prognostic experiments

The main input data along with flow-line profiles for the prognostic experiments, namely, the surface mass balance, are adopted from Bassford et al. (2006). Figure 7 shows the elevational mass-balance distribution along the C–C′ flow line, i.e. it shows how the surface mass balance changes with elevation in the C–C′ direction (Bassford et al., 2006). For the B–B′ and D–D′ flow lines, the elevational mass-balance distributions are qualitatively the same (Bassford et al., 2006). In the prognostic experiments that have been carried out, the mass balance is considered as time-independent. That is, the elevational mass-balance distributions are kept unchanged for the considered time period in the future. Thus, we intend to assess the maximum ice thickness in the ice streams in the future, because the forecasts implemented with the time-independent surface mass balance, do not imply a future global warming and, so, they do not suggest a future mass balance drift down into the ablation zone. Similarly, the ice surface temperature is suggested to be time-independent but dependent on elevation, i.e. according to Eq. (4), it is changed with elevation with a constant value of  $T_{s0}(t)$ . From the borehole temperature measurements, the present ice surface temperature at the summit is about  $-7.2^{\circ}\text{C}$ . The initial ice temperatures applied in the prognostic experiments are shown in Fig. 5.

Despite that future warming scenarios are not included into the prognostic experiments, the modeled ice cap response to the present environmental impact, which is reflected in the elevational mass-balance distribution (Bassford et al., 2006), reveals that the ice thicknesses gradually diminish along all the three flow lines. Figures 8a–

## Fast-flowing ice streams from the Academy of Sciences Ice Cap

Y. V. Konovalov and  
O. V. Nagornov

Title Page

Abstract

Introduction

Conclusions

References

Tables

Figures

◀

▶

◀

▶

Back

Close

Full Screen / Esc

Printer-friendly Version

Interactive Discussion



10a show the modeled successive ice surfaces divided into 50 year time intervals for the B–B′, C–C′, and D–D′ profiles, respectively. Figures 8b–10b show the same results as Figs. 8a–10a, respectively, but these complementary figures show the evolutions of the three ice shelves in more detail. The prognostic experiments are performed by applying a rectangular ice-shelf geometry. The cumulative impact of sea water, surface mass balance, and ice flow changes in the glacier has produced the future modeled ice shelf geometries. The ancillary black circles in Figs. 8–10 are aligned with the grid nodes and, thus, they show the spatial resolution, at which the prognostic experiments have been implemented. The spatial resolution is irregular and is about 100 m in the ice shelves and in the grounding line vicinity. The spatial grid is considered unchangeable throughout the period of the modeling.

The grounding line history, i.e. grounding line retreat or advance, specifically reflects the growing or diminishing ice mass, i.e. the history is an indicator of the glacier evolution. The grounding line retreats (a) along the B–B′ flow line from ~ 40 to ~ 30 km (Fig. 11a), (b) along the C–C′ flow line from ~ 43 to ~ 37 km (Fig. 11b), and (c) along the D–D′ flow line from ~ 41 to ~ 32 km (Fig. 11c) considering a time period of 500 years.

The ice flow velocities in the ice streams decrease with time and this trend diminishes the outgoing ice fluxes in the future. Figure 12 shows the modeled outgoing ice flux histories, i.e. it shows how the value  $\bar{u}Hb$ , which is defined at the ice-shelf terminus, changes with time. There are small peaks that periodically disturb main historical trends of the three outgoing ice fluxes. Every peak reflects ice calving at the ice-shelf terminus. Similarly, the ice calving provides a sudden change in the value of the outgoing ice flux ( $\bar{u}Hb$ ) due to a sudden change in the ice thickness ( $H$ ) at the terminus. Considering a complex environmental impact on ice shelves (Bassis et al., 2008), from the mathematical point of view it can be suggested that the calving processes are described by a stochastic model. Hence, the overall annual (or decadal) sizes of the anticipated ice debris can be described by a frequency distribution function. For convenience, the periodic calving of equal-size debris is considered herein, i.e.  $\delta$ -function is



Pattyn, 2000; Gudmundsson, 2011). Hence, the friction coefficient inversion performed for the three cross-sections can be interpreted as follows:

1. A large value of the friction coefficient at  $0 \text{ km} < x < 20 \text{ km}$  apparently means that ice is frozen to the bed at these distances from the summit. Then, the basal temperature increases at  $25 \text{ km} < x < 40 \text{ km}$  and the basal sliding at sub-freezing temperatures can appear due to the existence of a layer of ice-laden subglacial drift (Echelmeyer and Zhongxiang, 1987). Echelmeyer and Zhongxiang (1987) measured sliding rates of  $0.5 \text{ mm day}^{-1}$  over a solid rock surface at a temperature of  $-4.6^\circ\text{C}$  under a shear stress of approximately 60 kPa. This sliding rate can provide the ice surface velocity of about  $180\text{--}200 \text{ m a}^{-1}$ , and thus can explain the fast-flowing ice streams.

Otherwise, it seems that the basal temperature can reach the melting point at  $25 \text{ km} < x < 40 \text{ km}$  due to an increase in both deformational heating and ice surface temperature (e.g. Pattyn et al., 2005). Thus, the basal sliding can appear at  $x > 25 \text{ km}$  due to the regelation mechanism (Weertman, 1957; Li et al., 2010). In addition, the presence of water in the basal layer can be explained by the low bed elevations in the areas of fast-flowing ice streams (e.g. Knight, 1999; Vieli et al., 2001) or by a hydrological processes (e.g. Röthlisberger, 1972; Nye, 1976; Hewitt, 2011; Hoffman and Price, 2014). The presence of water in the basal layer provides the basal sliding which with time increases the basal temperature from the basal friction in the appropriate areas of the ice base.

2. In addition, the two evidently distinguished levels in the inverted friction coefficient distributions can be explained by changing the physical properties of the bedrock along the flow lines. Similarly, the large values of the friction coefficient at  $0 \text{ km} < x < 20 \text{ km}$  justify the rock-type bottom where ice is frozen to the bed (the ice temperature at  $0 \text{ km} < x < 20 \text{ km}$  is lower than the melting point). The lower values of the friction coefficient at  $25 \text{ km} < x < 40 \text{ km}$  presumably indicate the existence of the till layer at the bottom (e.g. Engelhardt et al., 1978, 1979; Boulton,

**Fast-flowing ice streams from the Academy of Sciences Ice Cap**

Y. V. Konovalov and  
O. V. Nagornov

Title Page

Abstract

Introduction

Conclusions

References

Tables

Figures



Back

Close

Full Screen / Esc

Printer-friendly Version

Interactive Discussion





## Fast-flowing ice streams from the Academy of Sciences Ice Cap

Y. V. Konovalov and  
O. V. Nagornov

Title Page

Abstract

Introduction

Conclusions

References

Tables

Figures

◀

▶

◀

▶

Back

Close

Full Screen / Esc

Printer-friendly Version

Interactive Discussion



variability in the inverted friction coefficients obtained for both the linear and nonlinear friction laws (Konovalov, 2012) implies that the physical properties of the basal layer change according to the friction coefficient distribution along the flow line. In particular, the water content in the basal layer can vary in agreement with the bed elevation changes, and the enhancement of water content at lower elevations provides a decrease in the friction coefficient in the corresponding areas.

Finally, two areas can be distinguished in the ice base, where basal ice is frozen to the bed ( $0 \text{ km} < x < 20 \text{ km}$ ) and where there is basal sliding ( $25 \text{ km} < x < 40 \text{ km}$ ). The boundary of transition from the area of the frozen basal ice to the area of the basal sliding is diluted due to smoothing of the inverted friction coefficient by the stabilizer. The linear friction law provides a good agreement between the observed and modeled surface velocity distributions along the flow line. Thus, it can be conveniently applied in the applications (in particular, in the prognostic experiments).

The prognostic experiments reveal that both ice mass and ice stream extents decline for the reference time-independent mass balance (Bassford et al., 2006). These experiments demonstrate that the grounding lines have retreated at about 10 km for the three ice streams considering a time period of 500 years and a steady-state environmental impact. The ice flow velocities in the ice streams decrease with time due to (a) diminishing of ice thicknesses and (b) retreating of the grounding lines from the sliding zones toward the zones where ice is frozen to the bed (inverted friction coefficient distributions are considered as time-independent). Thus, the maxima of the ice flow velocities in the ice streams decrease from  $\sim 80\text{--}120$  to  $\sim 20\text{--}30 \text{ ma}^{-1}$ . These trends in the ice flow velocities diminish the outgoing ice fluxes and as a result diminish the overall ice flux. Generally, the modeled histories are in agreement with the observations of sea ice extent and thickness indicating a continual ice decline in the Arctic.

## 5 Conclusions

The modeled present ice temperatures (Fig. 5) are qualitatively the same in the three cross-sections. There are resembling zones of relatively cold ice that can be distinguished in the modeled temperatures in the middle of the cross-sections. These cold ice zones reflected the surface temperature minimum about 150–200 years ago in the inverted past temperature history (Nagornov et al., 2005, 2006). This surface temperature minimum corresponds to an event that is known as Little Ice Age.

The inversions of the friction coefficient performed for the three cross-sections can be interpreted as follows. The two levels that are evidently distinguished in the inverted friction coefficient distributions (Fig. 6) can be explained by changing the physical properties of the bedrock along the flow lines. Similarly, the large values of the friction coefficient at  $0 \text{ km} < x < 20 \text{ km}$  justify the rock-type bottom where ice is frozen to the bed (the ice temperature at  $0 \text{ km} < x < 20 \text{ km}$  is lower than the melting point). The lower values of the friction coefficient at  $25 \text{ km} < x < 40 \text{ km}$  presumably indicate the existence of the till layer (or the sandy layer) at the bottom. Specifically, the till layer provides the basal ice sliding.

The prognostic experiments carried out with the reference mass balance (Bassford et al., 2006) show that the grounding line has been retreated at about 10 km in the three ice streams considering a time period of 500 years. Similarly, the grounding line retreats (a) along the C–C' flow line from  $\sim 43$  to  $\sim 37$  km (the distance from the summit), (b) along the B–B' flow line from  $\sim 40$  to  $\sim 30$  km, and (c) along the D–D' flow line from  $\sim 41$  to  $\sim 32$  km considering a time period of 500 years and assuming time-independent mass balance. In the experiments, the ice flow velocities in the ice streams decrease with time due to (a) diminishing of the ice thicknesses and (b) retreating of the grounding lines from the sliding zones toward the zones where ice is frozen to the bed. Thus, the maxima of the ice flow velocities in the ice streams decrease from  $\sim 80$ – $120$  to  $\sim 20$ – $30 \text{ m a}^{-1}$ . These trends in the ice flow velocities diminish the outgoing ice fluxes and as a result diminish the overall ice flux. Generally, the modeled histories are

# ESDD

6, 2211–2242, 2015

## Fast-flowing ice streams from the Academy of Sciences Ice Cap

Y. V. Konovalov and  
O. V. Nagornov

Title Page

Abstract

Introduction

Conclusions

References

Tables

Figures

◀

▶

◀

▶

Back

Close

Full Screen / Esc

Printer-friendly Version

Interactive Discussion

in agreement with the observations of sea ice extent and thickness indicating a continual ice decline in the Arctic.

*Acknowledgements.* The authors are grateful to J. A. Dowdeswell et al. for the data that have been used in the manuscript. The authors are grateful to F. Pattyn for useful comments to the manuscript.

## References

Arkipov, S. M.: Data Bank “Deep drilling of glaciers: Soviet-Russian Projects in Arctic, 1975–1990”, *Data Glaciol. Stud.*, 87, 229–238, 1999.

Arthern, R. and Gudmundsson, H.: Initialization of ice-sheet forecasts viewed as an inverse Robin problem, *J. Glaciol.*, 56, 527–533, 2010.

Bassford, R. P., Siegert, M. J., Dowdeswell, J. A., Oerlemans, J., Glazovsky, A. F., and Macheret, Y. Y.: Quantifying the mass balance of ice caps on Severnaya Zemlya, Russian High Arctic I: Climate and mass balance of the Vavilov Ice Cap, *Arct. Antarct. Alp. Res.*, 38, 1–12, 2006.

Bassis, J. N., Fricker, H. A., Coleman, R., and Minster, J.-B.: An investigation into the forces that drive ice-shelf rift propagation on the Amery Ice Shelf, East Antarctica, *J. Glaciol.*, 54, 17–27, 2008.

Cuffey, K. and Paterson, W. S. B.: *The Physics of Glaciers*, 4th Edn., Butterworth-Heinemann, Oxford, 2010.

Bindschadler, R.: The importance of pressurized subglacial water in separation and sliding at the glacier bed, *J. Glaciol.*, 29, 3–19, 1983.

Boulton, G. S.: Processes of glacier erosion on different substrata, *J. Glaciol.*, 23, 15–38, 1979.

Boulton, G. S. and Jones, A. S.: Stability of temperate ice caps and ice sheets resting on beds of deformable sediment, *J. Glaciol.*, 24, 29–43, 1979.

Budd, W. E., Keage, P. L., and Blundy, N. A.: Empirical studies of ice sliding, *J. Glaciol.*, 23, 157–170, 1979.

Colinge, J. and Blatter, H.: Stress and velocity fields in glaciers: Part I. Finite difference schemes for higher-order glacier models, *J. Glaciol.*, 44, 448–456, 1998.

Dowdeswell, J. A., Bassford, R. P., Gorman, M. R., Williams, M., Glazovsky, A. F., Macheret, Y. Y., Shepherd, A. P., Vasilenko, Y. V., Savatyugin, L. M., Hubberten, H. W., and

## Fast-flowing ice streams from the Academy of Sciences Ice Cap

Y. V. Konovalov and  
O. V. Nagornov

Title Page

Abstract

Introduction

Conclusions

References

Tables

Figures

◀

▶

◀

▶

Back

Close

Full Screen / Esc

Printer-friendly Version

Interactive Discussion



## Fast-flowing ice streams from the Academy of Sciences Ice Cap

Y. V. Konovalov and  
O. V. Nagornov

Title Page

Abstract

Introduction

Conclusions

References

Tables

Figures

◀

▶

◀

▶

Back

Close

Full Screen / Esc

Printer-friendly Version

Interactive Discussion



Miller, H.: Form and flow of the Academy of Sciences Ice Cap, Severnaya Zemlya, Russian High Arctic, *J. Geophys. Res.*, 107, 1–15, 2002.

Echelmeyer, K. and Zhongxiang, W.: Direct observation of basal sliding and deformation of basal drift at sub-freezing temperatures, *J. Glaciol.*, 33, 83–98, 1987.

5 Engelhardt, H. F. and Kamb, B.: Basal sliding of Ice Stream B, West Antarctica, *J. Glaciol.*, 544, 223–230, 1998.

Engelhardt, H. F., Harrison, W. D., and Kamb, B.: Basal sliding and conditions at the glacier bed as revealed by bore-hole photography, *J. Glaciol.*, 20, 469–508, 1978.

10 Engelhardt, H. F., Kamb, B., Raymond, C. F., and Harrison, W. D.: Observation of basal sliding of variegated glacier, Alaska, *J. Glaciol.*, 23, 406–407, 1979.

Gagliardini, O., Jay-Allemand, M., and Gillet-Chaulet, F.: Friction distribution at the base of a surging glacier inferred from an inverse method, AGU Fall Meeting, 13–17 December 2010, San Francisco, CA, USA, Abstract: C13A-0540, 2010.

15 Gudmundsson, G. H.: Ice-stream response to ocean tides and the form of the basal sliding law, *The Cryosphere*, 5, 259–270, doi:10.5194/tc-5-259-2011, 2011.

Habermann, M., Maxwell, D. A., and Truffer, M.: A principled stopping criterion for the reconstruction of basal properties in ice sheets, AGU Fall Meeting, 13–17 December 2010, San Francisco, CA, USA, Abstract: C21C-0556, 2010.

20 Hewitt, I. J.: Modelling distributed and channelized subglacial drainage. The spacing of channels, *J. Glaciol.*, 57, 302–314, doi:10.3189/002214311796405951, 2011.

Hoffman, M. and Price, S.: Feedbacks between coupled subglacial hydrology and glacier dynamics, *J. Geophys. Res.-Earth*, 119, 414–436, doi:10.1002/2013JF002943, 2014.

Iken, A.: The effect of the subglacial water pressure on the sliding velocity of a glacier in an idealized numerical model, *J. Glaciol.*, 27, 407–421, 1981.

25 Jansson, P.: Water pressure and basal sliding on Storglaciären, northern Sweden, *J. Glaciol.*, 41, 232–240, 1995.

Jay-Allemand, M., Gillet-Chaulet, F., Gagliardini, O., and Nodet, M.: Investigating changes in basal conditions of Variegated Glacier prior to and during its 1982–1983 surge, *The Cryosphere*, 5, 659–672, doi:10.5194/tc-5-659-2011, 2011.

30 Knight, P. G.: *Glaciers*, Stanley Thornes, Cheltenham, UK, 1999.

Konovalov, Y. V.: Inversion for basal friction coefficients with a two-dimensional flow line model using Tikhonov regularization, *Res. Geophys.*, 2, 82–89, 2012.

---

## Fast-flowing ice streams from the Academy of Sciences Ice Cap

Y. V. Konovalov and  
O. V. Nagornov

---

[Title Page](#)[Abstract](#)[Introduction](#)[Conclusions](#)[References](#)[Tables](#)[Figures](#)[◀](#)[▶](#)[◀](#)[▶](#)[Back](#)[Close](#)[Full Screen / Esc](#)[Printer-friendly Version](#)[Interactive Discussion](#)

Larour, E., Seroussi, H., Morlighem, M., and Rignot, E.: Continental scale, high order, high spatial resolution, ice sheet modeling using the Ice Sheet System Model (ISSM), *J. Geophys. Res.*, 117, 1–20, 2012.

Leonov, A. S.: Some a posteriori termination rules for the iterative solution of linear ill-posed problems, *Comp. Math. Math. Phys.*, 34, 121–126, 1994.

Li, X., Sun, B., Siegert, M. J., Bingham, R. G., Tang, X., Zhang, D., Cui, X., and Zhang, X.: Characterization of subglacial landscapes by a two-parameter roughness index, *J. Glaciol.*, 56, 831–836, 2010.

MacAyeal, D. R.: Large-scale ice flow over a viscous basal sediment: theory and application to ice stream B, Antarctica, *J. Geophys. Res.*, 94, 4071–4088, 1989.

MacAyeal, D. R.: The basal stress-distribution of Ice Stream-E, Antarctica, inferred by control methods, *J. Geophys. Res.-Sol. Ea.*, 97, 595–603, 1992.

Morlighem, M., Rignot, E., Seroussi, H., Larour, E., Ben Dhia, H. and Aubry, D.: Spatial patterns of basal drag inferred using control methods from a full-Stokes and simpler models for Pine Island Glacier, West Antarctica, *Geophys. Res. Lett.*, 37, L14502, doi:10.1029/2010GL043853, 2010.

Nagornov, O. V., Konovalov, Y. V., and Tchijov, V.: Reconstruction of past temperatures for Arctic glaciers subjected to intense subsurface melting, *Ann. Glaciol.*, 40, 61–66, 2005.

Nagornov, O. V., Konovalov, Y. V., and Tchijov, V.: Temperature reconstruction for Arctic glaciers, *Palaeogeogr. Palaeoclimatol.*, 236, 125–134, 2006.

Nye, J. F.: Water flow in glaciers: jökulhlaups, tunnels and veins, *J. Glaciol.*, 17, 181–207, 1976.

Paterson, W. S. B. and Clarke, G. K. S.: Comparison of theoretical and observed temperatures profiles in Devon Island ice cap, Canada, *Geophys. J. Roy. Astr. Soc.*, 55, 615–632, 1978.

Pattyn, F.: Ice-sheet modeling at different spatial resolutions: focus on the grounding zone, *Ann. Glaciol.*, 31, 211–216, 2000.

Pattyn, F.: Transient glacier response with a higher-order numerical ice-flow model, *J. Glaciol.*, 48, 467–477, 2002.

Pattyn, F., De Brabander, S., and Huyghe, A.: Basal and thermal control mechanisms of the Ragnhild glaciers, East Antarctica, *Ann. Glaciol.*, 40, 225–231, doi:10.3189/172756405781813672, 2005.

Pattyn, F., Perichon, L., Aschwanden, A., Breuer, B., de Smedt, B., Gagliardini, O., Gudmundsson, G. H., Hindmarsh, R. C. A., Hubbard, A., Johnson, J. V., Kleiner, T., Konovalov, Y., Martin, C., Payne, A. J., Pollard, D., Price, S., Rückamp, M., Saito, F., Souček, O., Sugiyama, S.,

## Fast-flowing ice streams from the Academy of Sciences Ice Cap

Y. V. Konovalov and  
O. V. Nagornov

Title Page

Abstract

Introduction

Conclusions

References

Tables

Figures

◀

▶

◀

▶

Back

Close

Full Screen / Esc

Printer-friendly Version

Interactive Discussion



and Zwinger, T.: Benchmark experiments for higher-order and full-Stokes ice sheet models (ISMIP–HOM), *The Cryosphere*, 2, 95–108, doi:10.5194/tc-2-95-2008, 2008.

Röthlisberger H.: Water pressure in intra- and subglacial channels, *J. Glaciol.*, 11, 77–203, 1972.

- 5 Sergienko, O. V., Bindschadler, R. A., Vornberger, P. L., and MacAyeal, D. R.: Ice stream basal conditions from block-wise surface data inversion and simple regression models of ice stream flow: application to Bindschadler Ice Stream, *J. Geophys. Res.*, 113, 1–11, 2008.

Tikhonov, A. N. and Arsenin, V. I.: *Solutions of Ill Posed Problems*, Winston & Sons, Washington, 1977.

- 10 Van der Veen, C. J.: Longitudinal stresses and basal sliding: a comparative study, in: *Dynamics of the West Antarctic Ice Sheet*, edited by: Van der Veen, C. J. and Oerlemans, J., D. Reidel Publishing Co., Dordrecht, 223–248, 1987.

Vieli, A., Funk, M., and Blatter, H.: Flow dynamics of tidewater glaciers: a numerical modelling approach, *J. Glaciol.*, 47, 595–606, 2001.

- 15 Weertman, J.: On the sliding of glaciers, *J. Glaciol.*, 3, 33–38, 1957.

Zagorodnov, V. S.: Recent Soviet activities on ice core drilling and core investigations in Arctic region, *Bull. Glacier Res.*, 6, 81–84, 1988.

## Fast-flowing ice streams from the Academy of Sciences Ice Cap

Y. V. Kononov and  
O. V. Nagornov



**Figure 1.** After Dowdeswell et al. (2002). Map of Severnaya Zemlya showing the Academy of Sciences Ice Cap on Komsomolets Island together with the other ice caps in the archipelago: Rusanov Ice Cap, Vavilov Ice Cap, Karpinsky Ice Cap, University Ice Cap, Pioneer Glacier, Semenov-Tyan Shansky Glacier, Kropotkin Glacier, Leningrad Glacier. Inset is the location of Severnaya Zemlya and the nearby Russian Arctic archipelagos of Franz Josef Land and Novaya Zemlya within the Eurasian High Arctic.

Title Page

Abstract

Introduction

Conclusions

References

Tables

Figures

◀

▶

◀

▶

Back

Close

Full Screen / Esc

Printer-friendly Version

Interactive Discussion

## Fast-flowing ice streams from the Academy of Sciences Ice Cap

Y. V. Konovalov and  
O. V. Nagornov

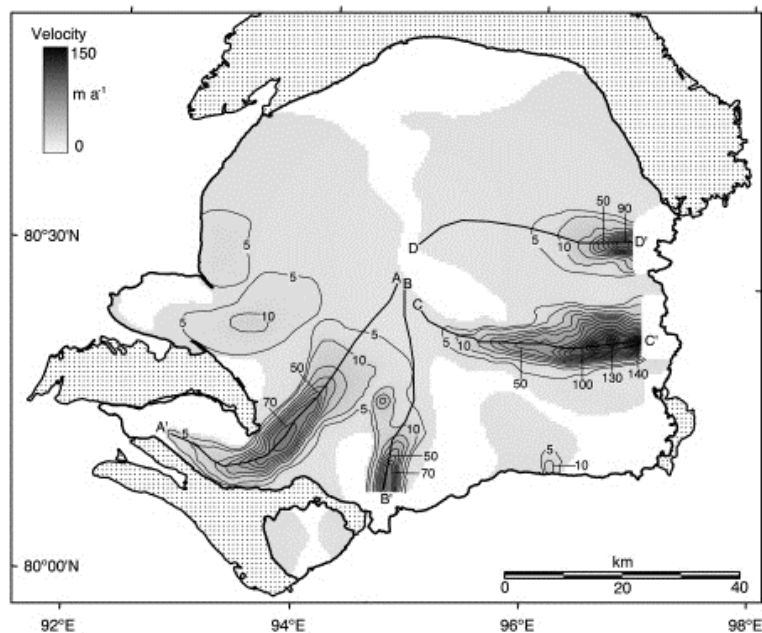


**Figure 2.** After Dowdeswell et al. (2002). Corrected interferometrically derived ice surface velocities for the Academy of Sciences Ice Cap. The first two contours are at velocities of  $5$  and  $10 \text{ m a}^{-1}$ , with subsequent contours at  $10 \text{ m a}^{-1}$  intervals. The unshaded areas of the ice cap are regions of non-corrected velocity data. The dotted areas represent bare land. The four fast flowing ice stream central lines are denoted as A–A', B–B', C–C', D–D', respectively. Velocity profiles A–A' to D–D' are shown in Fig. 11 of Dowdeswell et al. (2002)

Title Page

Abstract

Introduction

Conclusions

References

Tables

Figures

◀

▶

◀

▶

Back

Close

Full Screen / Esc

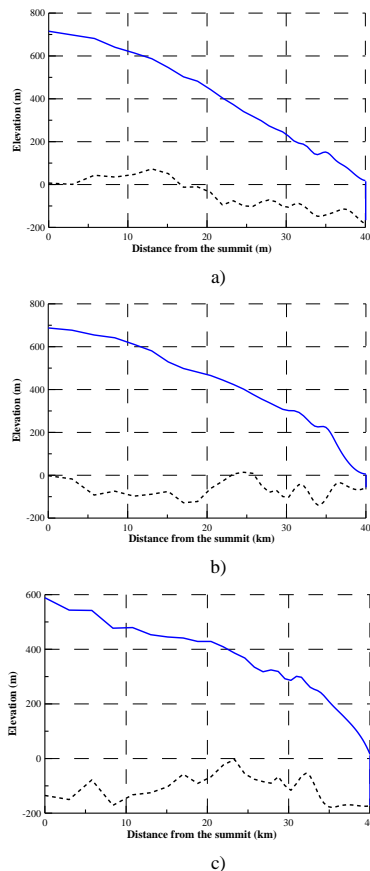
Printer-friendly Version

Interactive Discussion



## Fast-flowing ice streams from the Academy of Sciences Ice Cap

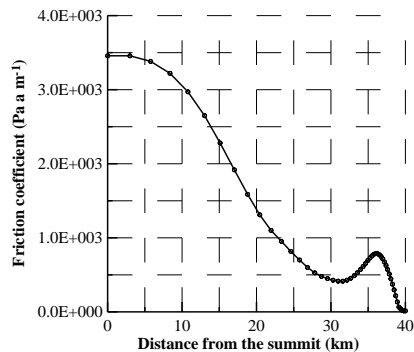
Y. V. Konovalov and  
O. V. Nagornov

[Title Page](#)[Abstract](#)[Introduction](#)[Conclusions](#)[References](#)[Tables](#)[Figures](#)[◀](#)[▶](#)[◀](#)[▶](#)[Back](#)[Close](#)[Full Screen / Esc](#)[Printer-friendly Version](#)[Interactive Discussion](#)

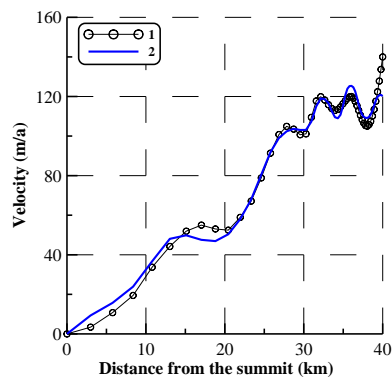
**Figure 3.** (a) B–B' flow line profile, which crosses downstream one of the four fast flowing ice streams in the Academy of Sciences Ice Cap (Fig. 2). (b) C–C' flow line profile. (c) D–D' flow line profile. The data of ice surface and ice bed elevations are imported from Fig. 8 of Dowdeswell et al. (2002).

## Fast-flowing ice streams from the Academy of Sciences Ice Cap

Y. V. Konovalov and  
O. V. Nagornov



a)



b)

**Figure 4.** (a) The friction coefficient distribution are obtained in the inverse problem for *the linear friction law* and for the observed surface velocity distribution along the C–C' flow line. (b) The ice surface horizontal velocity distributions along the flow line: 1 – the observed surface velocity distribution, taken from Fig. 11 of Dowdeswell et al. (2002), 2 – the modeled surface velocity distribution, which corresponds to the reconstructed friction coefficient in Fig. 4a.

[Title Page](#)
[Abstract](#)
[Introduction](#)
[Conclusions](#)
[References](#)
[Tables](#)
[Figures](#)
[◀](#)
[▶](#)
[◀](#)
[▶](#)
[Back](#)
[Close](#)
[Full Screen / Esc](#)
[Printer-friendly Version](#)
[Interactive Discussion](#)

## Fast-flowing ice streams from the Academy of Sciences Ice Cap

Y. V. Konovalov and  
O. V. Nagornov

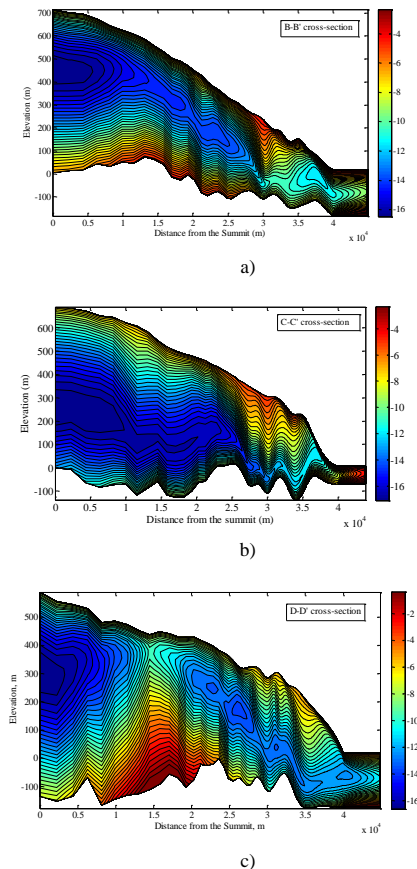


**Figure 5.** The temperature distributions within **(a)** the B–B' cross-section, **(b)** C–C' cross-section and **(c)** D–D' cross-section simulated by the model with the past surface temperature history based on the paleo-temperature, which is retrieved from the borehole temperature data (Nagornov et al., 2005, 2006).

## Fast-flowing ice streams from the Academy of Sciences Ice Cap

Y. V. Konovalov and  
O. V. Nagornov

Title Page

Abstract

Introduction

Conclusions

References

Tables

Figures

◀

▶

◀

▶

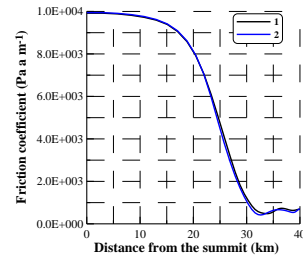
Back

Close

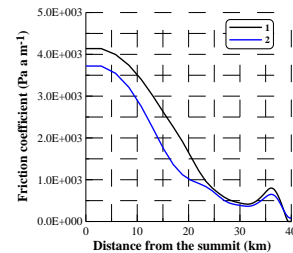
Full Screen / Esc

Printer-friendly Version

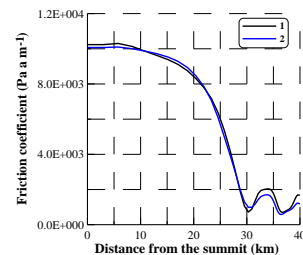
Interactive Discussion



a)

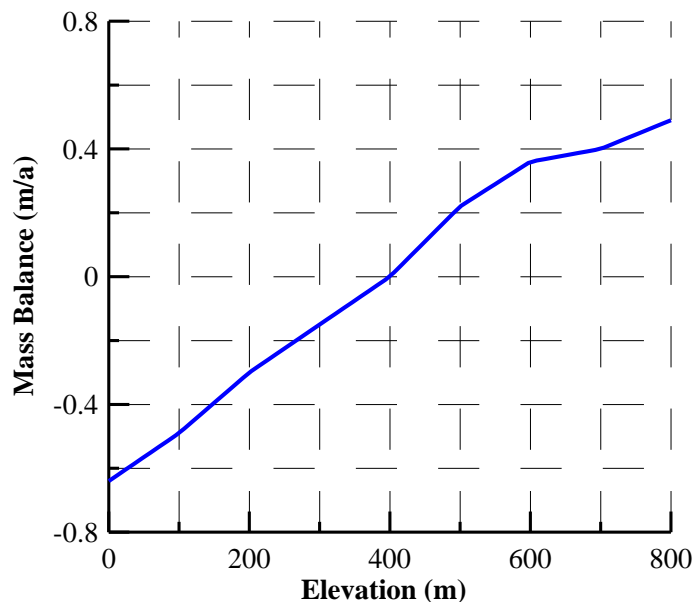


b)



c)

**Figure 6.** The friction coefficients inverted along **(a)** B–B' flow line, **(b)** C–C' flow line and **(c)** D–D' flow line. Curve 1 is the first inversion, which is obtained for the linear ice temperature profiles (the ice temperature approximation for the initial inversions). Curve 2 is the second inversion, which corresponds to the modeled ice temperature (Fig. 5).

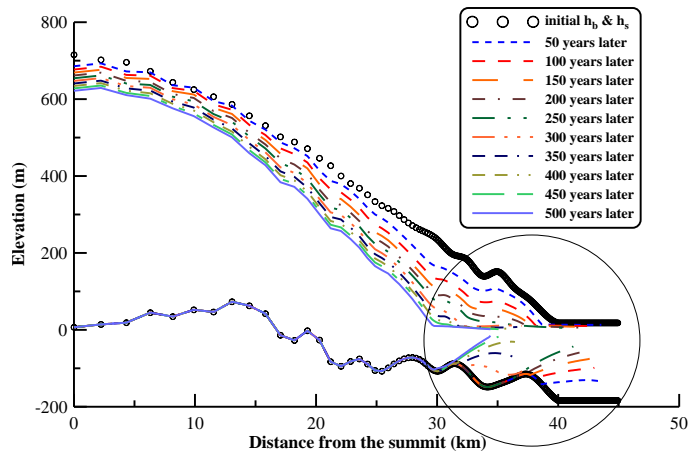
**Fast-flowing ice streams from the Academy of Sciences Ice Cap**Y. V. Konovalov and  
O. V. Nagornov

**Figure 7.** The surface mass balance elevational distribution along the C–C′ flow line (Bassford et al., 2006).

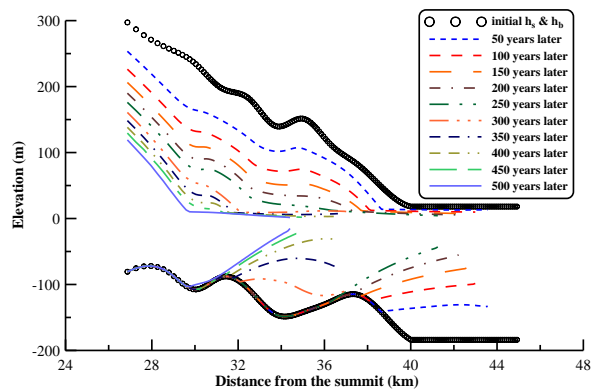
[Title Page](#)[Abstract](#)[Introduction](#)[Conclusions](#)[References](#)[Tables](#)[Figures](#)[◀](#)[▶](#)[◀](#)[▶](#)[Back](#)[Close](#)[Full Screen / Esc](#)[Printer-friendly Version](#)[Interactive Discussion](#)

## Fast-flowing ice streams from the Academy of Sciences Ice Cap

Y. V. Konovalov and  
O. V. Nagornov



a)

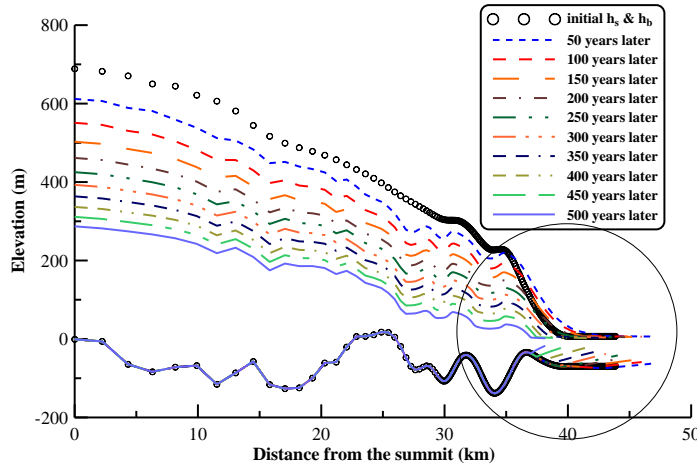


b)

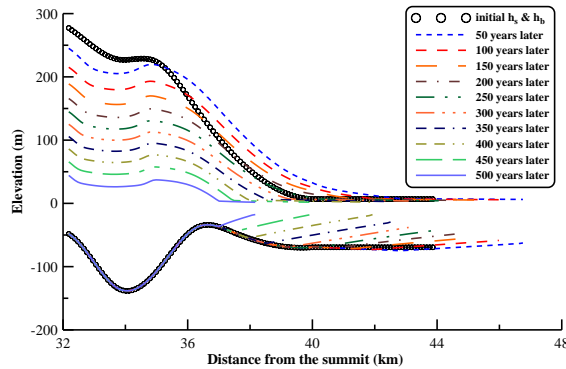
**Figure 8.** (a) The modeled successive B–B′ cross-section geometries separated by 50 year intervals from the present to the future 500 years later. (b) A magnified section of (a), showing the evolution of B–B′ ice shelf.

**Fast-flowing ice streams from the Academy of Sciences Ice Cap**

Y. V. Konovalov and  
O. V. Nagornov



a)



b)

**Figure 9.** (a) The modeled successive C–C' cross-section geometries separated by 50 year intervals from the present to the future 500 years later. (b) A magnified section of (a), showing the evolution of C–C' ice shelf.

Title Page

Abstract Introduction

Conclusions References

Tables Figures

◀ ▶

◀ ▶

Back Close

Full Screen / Esc

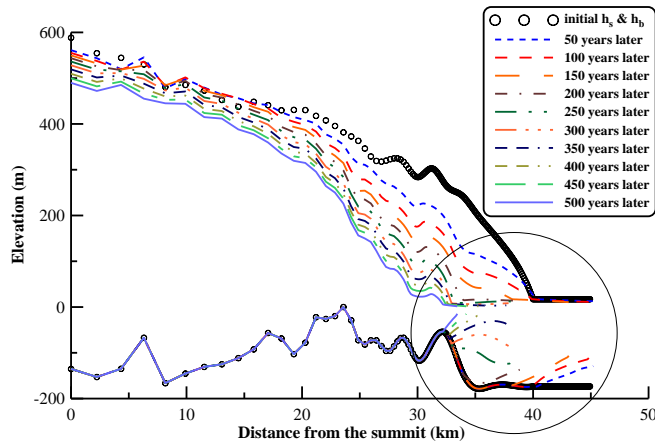
Printer-friendly Version

Interactive Discussion

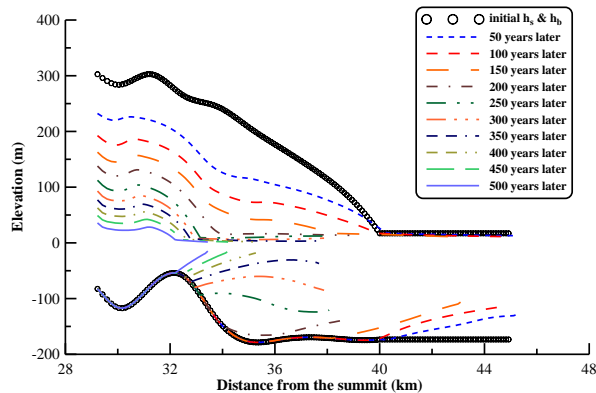


**Fast-flowing ice streams from the Academy of Sciences Ice Cap**

Y. V. Konovalov and  
O. V. Nagornov



a)



b)

**Figure 10. (a)** The modeled successive D–D′ cross-section geometries separated by 50 year intervals from the present to the future 500 years later. **(b)** A magnified section of **(a)**, showing the evolution of D–D′ ice shelf.

Title Page

Abstract Introduction

Conclusions References

Tables Figures

◀ ▶

◀ ▶

Back Close

Full Screen / Esc

Printer-friendly Version

Interactive Discussion



## Fast-flowing ice streams from the Academy of Sciences Ice Cap

Y. V. Konovalov and  
O. V. Nagornov

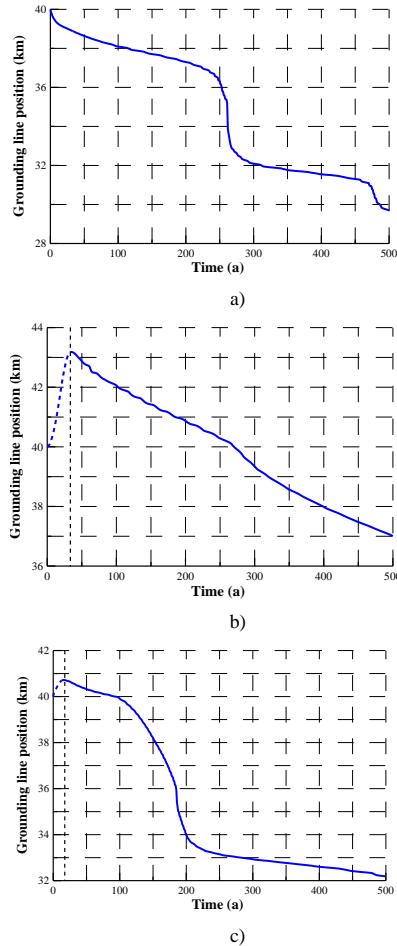


**Figure 11.** The modeled grounding line history **(a)** for B–B′ cross section **(b)** for C–C′ and **(c)** for D–D′ cross section.

Title Page	
Abstract	Introduction
Conclusions	References
Tables	Figures
◀	▶
◀	▶
Back	Close
Full Screen / Esc	
Printer-friendly Version	
Interactive Discussion	



## Fast-flowing ice streams from the Academy of Sciences Ice Cap

Y. V. Konovalov and  
O. V. Nagornov

Title Page

Abstract

Introduction

Conclusions

References

Tables

Figures

◀

▶

◀

▶

Back

Close

Full Screen / Esc

Printer-friendly Version

Interactive Discussion

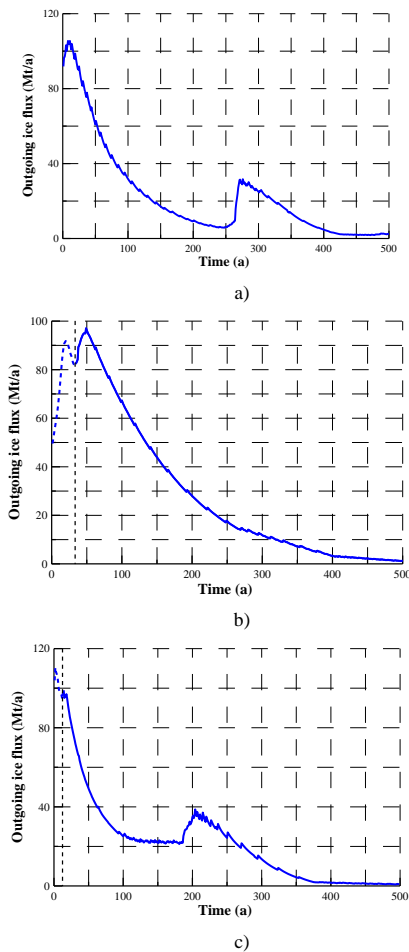


**Figure 12.** The modeled outgoing ice flux history (a) for B–B′ cross section (b) for C–C′ and (c) for D–D′ cross section.

---

## Fast-flowing ice streams from the Academy of Sciences Ice Cap

Y. V. Konovalov and  
O. V. Nagornov

---

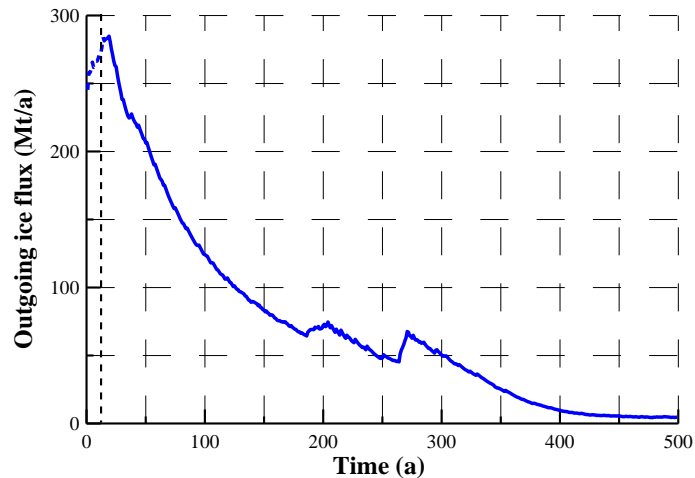


**Figure 13.** The overall outgoing ice flux history (the sum of the outgoing fluxes for the three ice streams: B–B', C–C' and D–D').

[Title Page](#)[Abstract](#)[Introduction](#)[Conclusions](#)[References](#)[Tables](#)[Figures](#)[◀](#)[▶](#)[◀](#)[▶](#)[Back](#)[Close](#)[Full Screen / Esc](#)[Printer-friendly Version](#)[Interactive Discussion](#)